AIAA JOURNAL
Vol. 36, No. 5, May 1998

High-Speed Turbulent Separated Flows: Consistency of Mathematical Models and Flow Physics

David S. Dolling*
University of Texas at Austin, Austin, Texas 78712

A large fraction of the experimental database used for validation of computational fluid dynamics (CFD) predictions of shock-induced turbulent separated flows consists of time-averaged measurements. If meaningful conclusions are to be drawn from comparisons of these time-averaged data with computations, it is important to understand how the data are generated physically. This can be difficult and time consuming but is an essential element in the selection of an appropriate mathematical model for the computation. For the separated compression ramp interaction, which is widely used as a CFD test case, global unsteadiness is a dominant phenomenon. Without modeling the unsteadiness, accurate predictions of the time-averaged wall pressure, outgoing velocity profiles, and other parameters will likely remain elusive, irrespective of the turbulence model.

Nomenclature

D	= fin leading-edge diameter
L_s	= length of separated flow
M	= Mach number
P	= pressure
P_t	= pitot pressure
q, Q	= heating rate
Re	= Reynolds number
S, R	= separation and reattachment locations
S, X	= streamwise distance from ramp corner (Fig. 1)
T	= temperature
Y	= distance above surface (Fig. 1)
Z	= distance perpendicular to ramp
α	= ramp corner angle
γ	= separation shock intermittency
δ	= boundary-layer thickness
θ	= shock generator angle
σ	= standard deviation

Subscripts

E/A	= ensemble averaged
max	= maximum value
w	= measured at wall
∞	= freestream condition

Superscript

-	= mean value

Introduction

AS a preface to the remarks made in this paper, note that the author is not an expert in computational fluid dynamics (CFD) nor has he participated to any great extent in the recent development of standards for establishing the credibility of CFD simulations. For discussion of the relevant issues and concerns, the reader is referred to Mehta,[1] who has recently prepared a "Guide to Credible Computer Simulations of Fluid Flows." Mehta presents 49 references dealing with a broad range of issues from verification, through validation, to certification. The focus of the current paper is on validation. According to Mehta,

> Validation is defined as the process of assessing the credibility of the simulation model, within its domain of applicability, by determining whether the right simulation model is developed and by estimating the degree to which this model is an accurate representation of reality from the perspective of its intended uses.

In a "perspective on aerospace computational fluid dynamics," Jameson[2] writes,

> Code validation is increasingly being recognized as being vital to raising confidence in CFD use. In considering this requirement, it is important to distinguish between the correctness of the program and the suitability of the math model to the application. Simply comparing experimental data with numerical results provides no way to distinguish the source of the discrepancies, whether they are due to faulty numerical approximation or programming, or to deviations between the math model and the true physics.

To determine whether such deviations exist, it is obviously necessary to understand what the true physics of the flowfield in question actually are. The intent of this paper is to illustrate, through example, how in certain cases time-averaged data alone can mask the true physics. The primary example used to bring out this point is the high-speed turbulent flow over an unswept ramp. For two-dimensional compression ramp flows at supersonic speed, the generally accepted model of the flowfield is shown in Fig. 1. This was determined by Settles[3] from pitot pressure, static pressure, and total temperature surveys. The separation and reattachment points were determined from kerosene-lampblack surface flow patterns. All of the measuring techniques have essentially zero frequency response, and so this model represents a time-averaged picture.

This flow was selected because of the experiences of the author and his awareness (often belated) of the pitfalls of developing flowfield models from time-averaged experimental data. Compression ramp flows have been studied experimentally since the 1950s, and results from such experiments have been used for comparison with numerical work since the 1970s. The nominal two dimensionality permits relatively rapid computations, at least compared with fully three-dimensional flows, and thus the ramp interaction has often been used to evaluate turbulence models and solution algorithms. The examples presented underscore the importance of understanding what time-averaged experimental data represent physically and ensuring that the mathematical model does not ignore this physics.

Some Comparisons of CFD Predictions and Experimental Data

Figure 2 shows comparisons of the normalized wall pressure from computations and experiment for turbulent flow over a 34-deg compression ramp at Mach 9.22. The data are those of Coleman[4] and Coleman and Stollery,[5] and the computations were made by Horstman[6] using the k–ε, Cebeci–Smith, and Baldwin–Lomax turbulence models. The computations employ the time-dependent,

Received Oct. 22, 1996; revision received May 21, 1997; accepted for publication June 2, 1997.

*Professor, Center for Aeromechanics Research. Associate Fellow AIAA.

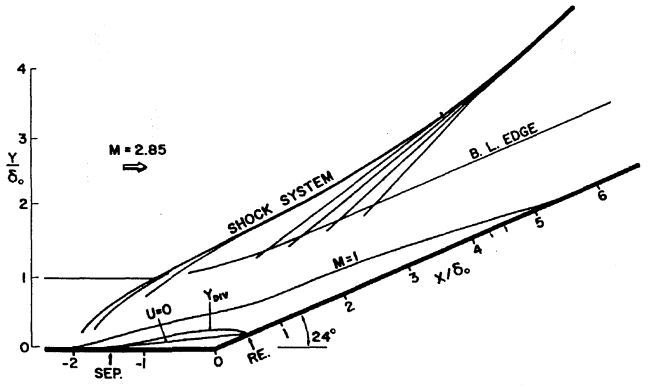

Fig. 1 Compression ramp flowfield model (figure from Ref. 3).

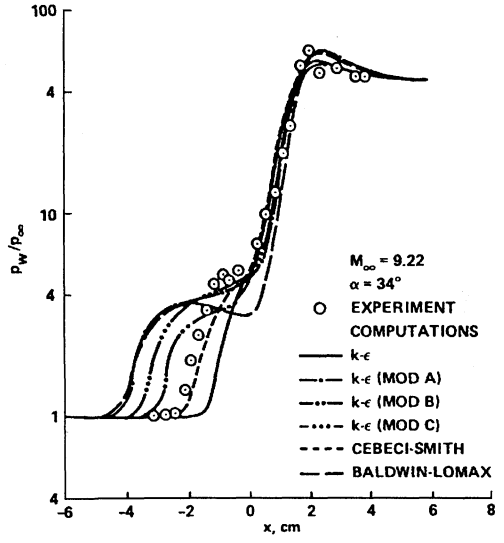

Fig. 2 Normalized wall pressure distributions in a compression ramp flow (figure from Ref. 6).

mass-weighted, Reynolds-averaged, Navier–Stokes equations for two-dimensional flow and are solved using the MacCormack explicit–implicit, second-order predictor–corrector, finite volume method. The purpose of Horstman's[6] study was to assess how well these turbulence models fare in hypersonic flows. It was not assumed, a priori, that they were suitable for hypersonic flow. Modifications to the k–ε model (indicated in the legend of Fig. 2) were made as follows: 1) Mod A is a correction to the ε equation to account for the effect of rapid compression on the turbulent length scale; 2) Mod B employs corrections to both the k and ε equations to model the additional terms, which appear after mass averaging; and 3) Mod C is a correction to the turbulent stress terms for the density fluctuations. Details are provided in Ref. 6.

Figure 3 shows comparisons of the same numerical approaches with the Mach 11.3 data of Holden.[7] The flowfield is generated by an incident shock wave generated by a wedge. In both the Mach 9 and 11 experiments, the wall temperature ratios are similar (T_w/T_0 = 0.28 and 0.19, respectively) and the Reynolds numbers differ only by a factor of two. In both cases, major discrepancies occur upstream of the ramp corner/shock impingement point. In Fig. 2 the Cebeci–Smith model predicts the wall pressure distribution quite well. The k–ε model underpredicts the upstream influence, whereas with Mods A, B, and C it is overpredicted. In contrast, at Mach 11 (Fig. 3) the Cebeci–Smith and k–ε models are now the worst, and the k–ε model with Mod C does the best. None of these predictions can be considered satisfactory upstream of the corner for the Mach 11 flow.

In Ref. 6 Horstman states, "Two features of shock wave boundary layer interaction flows which are probably of most interest to the designer are the maximum heat transfer near reattachment and the length of the separation zone." Comparisons of the measured and predicted values of (q_{max}/q_∞) and the separation locations are shown in Figs. 4 and 5, respectively, for the Mach 9.22 compression

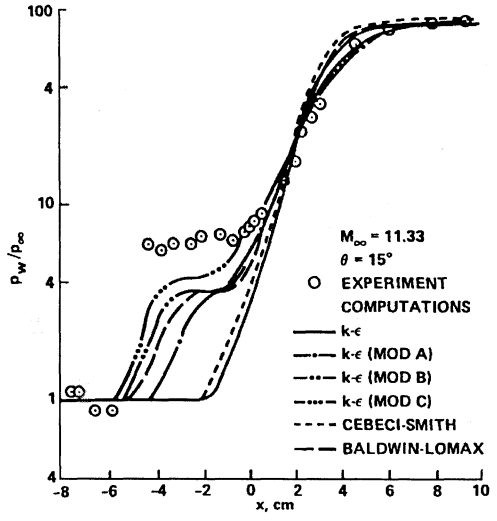

Fig. 3 Normalized wall pressure distributions in incident shock wave interaction (figure from Ref. 6).

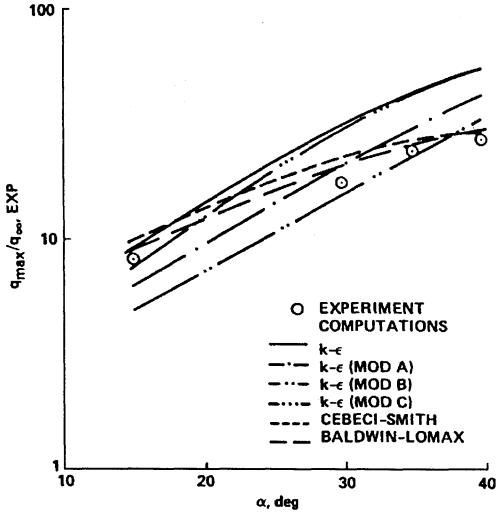

Fig. 4 Mach 9.22 compression ramp interaction: comparison of computed and experimental maximum heat transfer rates (figure from Ref. 6).

ramp experiment. Note that the vertical axis in Fig. 4 is logarithmic. The k–ε model and modifications overpredict the maximum heating for the separated cases ($\alpha > 30$ deg), whereas the algebraic models underpredict the separated cases. Figure 5 shows that the trends for the separation location are generally correct for all models, but only the Cebeci–Smith model predicts the values quantitatively. The latter result is fortuitous because similar comparisons at Mach 11 show that the Cebeci–Smith model is the worst. It is not just the maximum heating rate in the compression ramp interaction that is inadequately captured by any of the codes. The shape of the heat transfer rate distribution for both interactions is also poorly predicted.[6]

More recently, Coakley and Huang[8] have computed Coleman and Stollery's ramp flow using the Reynolds-averaged Navier–Stokes equations with mass-weighted averaging and several turbulence models. The latter included three k–ε models [Jones–Launder (JL), a model developed by Huang and Coakley based on results of direct numerical simulations (HC), and the So et al. model (SO)], as well as the k–ω model of Wilcox and the q–ω model of Coakley. Details are given in Ref. 8. The k–ε models of So et al. and Huang/Coakley, as given in Ref. 8, predicted the pressure distribution and separation length reasonably well, but none of the methods predicted the heating rate rise on the ramp face (Fig. 6a). Predicted peak heating exceeded the measurements by around 30% to almost 100%. Later computations of the same flow made by Coakley et al.[9] used corrected versions of the k–ε model of Jones–Launder (as modified by Launder and Sharma) and the k–ω model of Wilcox. Corrections

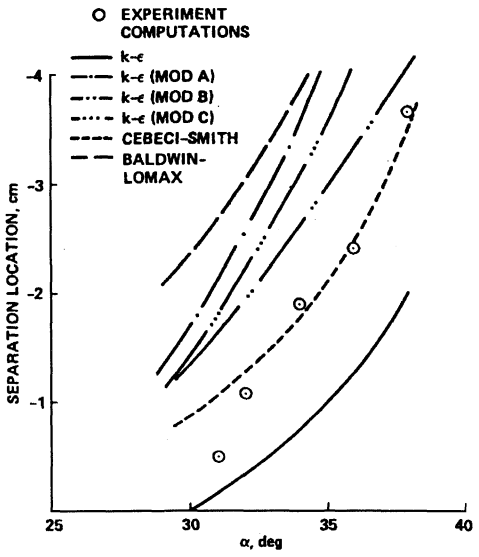

Fig. 5 Mach 9.22 compression ramp interaction: comparison of computed and experimental separation locations (figure from Ref. 6).

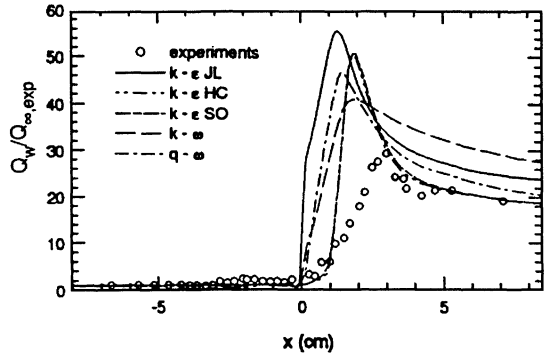

a) Comparison of computed and experimental heat transfer rates (figure from Ref. 8)

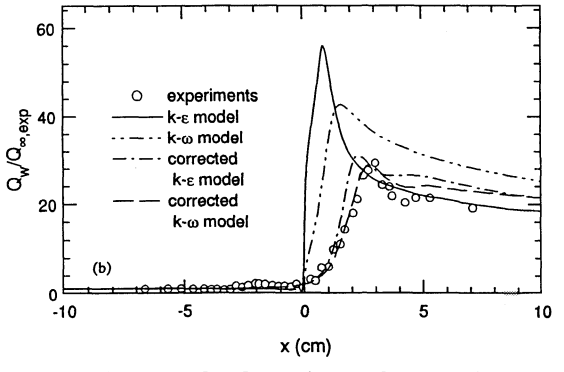

b) Comparison of computed and experimental heat transfer rate using corrected turbulence models (figure from Ref. 9)

Fig. 6 Mach 9.22 compression ramp interaction.

included a "length scale correction"[9] (which limits the slope of the length scale in the reattachment region) and a "rapid compression correction"[9] (which increases the production of ε or ω in regions of rapid compression, effectively reducing eddy viscosity and enhancing separation). Details are given in Ref. 9. The corrected models gave much better agreement with experiments, particularly for the heat transfer distribution. Peak heating on the ramp face was predicted very well (Fig. 6b).

Similar discrepancies are also seen at lower Mach numbers. Numerous computations, using a variety of turbulence models, have been made of the 24-deg, Mach 3 unswept compression ramp experiment of Settles.[3] Five sets of computed wall pressure distributions are shown in Fig. 7. Similar to the hypersonic results of Figs. 2 and 3, the major discrepancies are upstream of the corner.

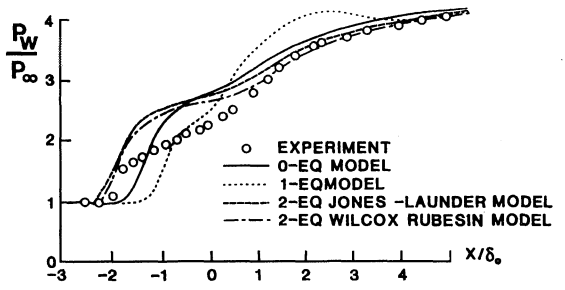

a) Viegas and Horstman[10]

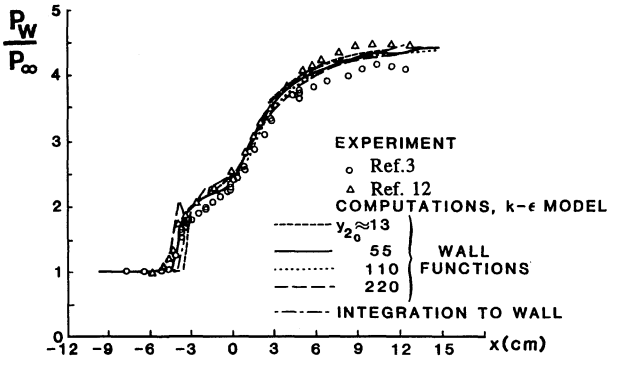

b) Viegas et al.[11]

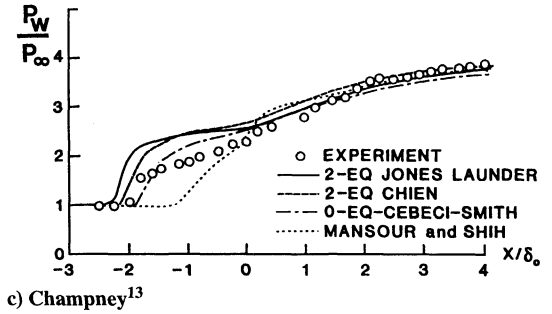

c) Champney[13]

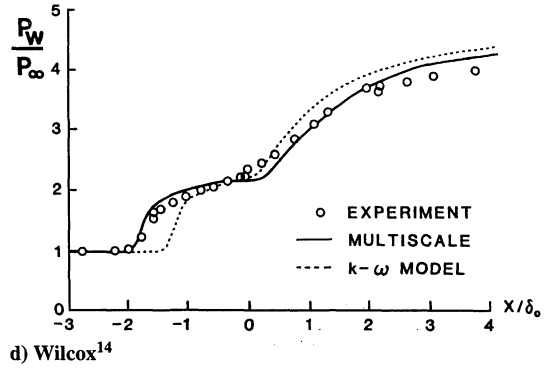

d) Wilcox[14]

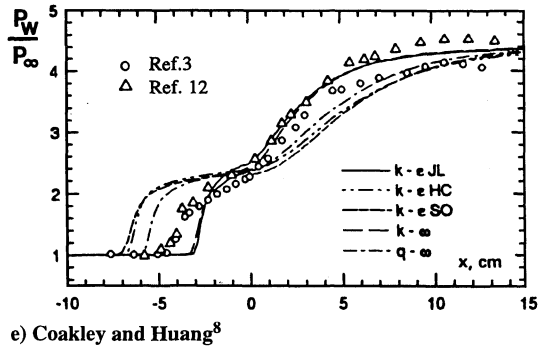

e) Coakley and Huang[8]

Fig. 7 Measured and computed wall pressure distributions in a 24-deg, Mach 3 compression ramp interaction.

Figure 7a shows those calculated by Viegas and Horstman[10] using turbulence models available in 1979; Fig. 7b shows these calculated by Viegas et al.[11] in 1985 using the k–ε model and employing both wall functions and integration to the wall (the experimental data of Dolling and Murphy[12] in Fig. 7b are time averages of fluctuating wall pressure signals rather than single-value mean measurements from scanivalves, as obtained by Settles[3]); Fig. 7c shows the results of Champney[13] presented in 1989, whereas Fig. 7d shows computations by Wilcox[14] in 1990, using his multiscale model and the k–ω model. Champney's work includes calculations made using the turbulence model of Mansour and Shih, which was derived from direct simulation data for a channel flow and applied for the first time to a compressible flow by Champney.[13] Coakley and Huang[8] have also calculated this flow using the same models used to compute the Coleman and Stollery ramp experiment (Fig. 7e).

The computations share certain common features: a generally steeper pressure gradient up through separation to the corner and a higher plateau level upstream of the corner than in the experiment. The k–ω model of Figs. 7d and 7e is an exception to the latter and predicts the plateau pressure fairly well, but the upstream influence is substantially underpredicted. Of all of the computations, Wilcox's multiscale model[14] seems superior; both upstream influence and plateau pressure levels are predicted quite well.

Horstman[6] also notes, "Experimenters have observed large unsteadiness for separated supersonic shock wave turbulent boundary layer interaction flows. There is no reason to doubt that unsteadiness is also present for the hypersonic test flows considered here. These unsteady effects can at times dominate the flowfield." He also pointed out that "the computations show no sign of unsteadiness. There is also no apparent mechanism in the present-day eddy viscosity models for the observed unsteadiness. This may be an important factor that contributes to the discrepancies between the predicted and measured results." That is certainly the case, and some of the effects of unsteadiness are discussed in the next three sections.

Time-Averaged Wall Pressures

The wall pressure in the experiment of Settles[3] was measured using the standard technique of wall tappings connected to a scanivalve via several feet of plastic tubing. The corresponding wall pressures are mean values. Measurements made in the same flowfield using high-frequency-response wall pressure transducers show that the distribution of the rms of the wall pressure fluctuations σp_w exhibits two peaks: one near separation and the other near reattachment (Fig. 8). The rms peak near separation is a common feature of many two- and three-dimensional, shock-induced turbulent separated flows.[15] The amplitude of the pressure fluctuations in this region is extremely large, with the maximum value of σp_w being a significant fraction of the local mean value $\bar{P}_w$. This large rise in rms is not due primarily to turbulence amplification through a nominally steady compression but is caused by unsteadiness of the separation shock wave. Wall pressure signals in this region show this very clearly (Fig. 9). The mean wall pressure $\bar{P}_w$ is indicated, and for reference, the incoming boundary-layer wall pressure signal is also shown. The

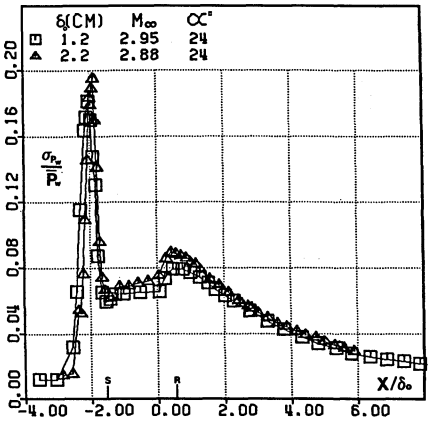

Fig. 8 Wall pressure standard deviation distributions in a 24-deg, Mach 3 compression ramp interaction (figure from Ref. 12).

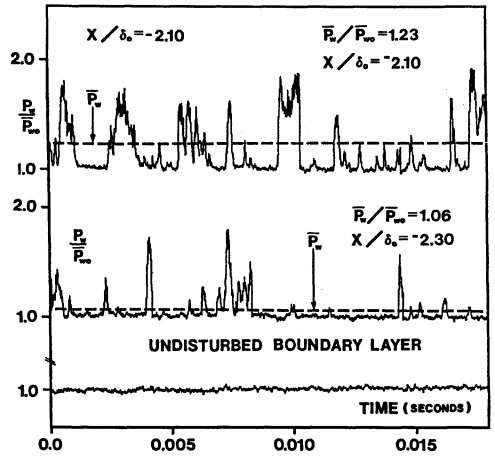

Fig. 9 Sample wall pressure signals upstream of separation in a 24-deg, Mach 3 compression ramp interaction (figure from Ref. 12).

instantaneous wall pressure P_w is intermittent, jumping randomly back and forth from the range characteristic of the undisturbed boundary layer to a higher level corresponding to flow downstream of the separation shock. The time-averaged wall pressure $\bar{P}_w$ is generated by the superposition of very large-amplitude fluctuations on the undisturbed boundary-layer pressure signal, and $\bar{P}_w$ increases in the downstream direction because the intermittency, i.e., the fraction of time that the separation shock wave spends upstream of the given station, progressively increases. The entire region upstream of the separation line S is characterized by an intermittent wall pressure signal. In the Mach 3 compression ramp flow, the length of the intermittent region, L_i, is about $0.75\delta_0$–$0.9\delta_0$ and represents the region over which $\bar{P}_w/\bar{P}_{w0}$ increases from about 1.0 to about 1.7.

Similar distributions of mean wall pressure and rms of the fluctuations have been measured in separated compression ramp interactions at Mach 5 (Ref. 15). Similar to the Mach 3 results cited, the intermittent region length scale is approximately $1\delta_0$. The maximum frequency of shock crossings over a given transducer in the intermittent region is about 1 kHz, which is typical of that measured in a wide variety of interactive flows under similar conditions.[15] Thus, this region of the flowfield is characterized by an unsteady separation shock whose motion is large scale and low frequency, i.e., low compared with the characteristic frequency of the incoming flow, U_∞/δ_0.

Erengil and Dolling[16] calculated ensemble-averaged $(\bar{P})_{E/A}$ pressures from the shock foot to the ramp corner, generated by freezing the shock at various positions in the intermittent region (Fig. 10). The symbol n represents the position of the shock in the intermittent region, and the solid line in Fig. 10 is the mean pressure distribution. Each one of the dashed-line curves was generated by freezing the shock at a given position in the intermittent region as it moved upstream and ensemble averaging on each of the downstream channels. Similar results were obtained for a downstream shock motion.

Three features are evident. First, $\bar{P}_{E/A}$ under the separated flow within about $1\delta_0$ upstream of the ramp corner is relatively insensitive to the shock position in the intermittent region. Second, for the shock-upstream case, the ensemble-averaged pressure distribution has a well-defined plateau region, consistent with a large-scale separated flow. Third, when the shock is at its most downstream position, the ensemble-averaged pressure distribution resembles that typical of a small-scale separated flow, i.e., no plateau region. Thus, the separated flow undergoes large, low-frequency, length-scale variations.

The only computations known to the author in which flowfield unsteadiness has been calculated are those of Hunt[17] and Hunt and Nixon.[18] A large eddy simulation of the 24 deg, Mach 3 ramp flow was performed. The simulation used a 117 × 61 × 59 grid (streamwise × spanwise × normal to wall), with the first grid point 0.015δ above the wall. This grid was considered "sufficient to model the largest eddies in the outer region of the boundary layer to allow the resolved turbulence to be self-sustaining."[18] The overall dimensions of the computational domain were 16δ streamwise, 5δ spanwise, and 3δ above the wall. The turbulence modeling research code (TMRC)

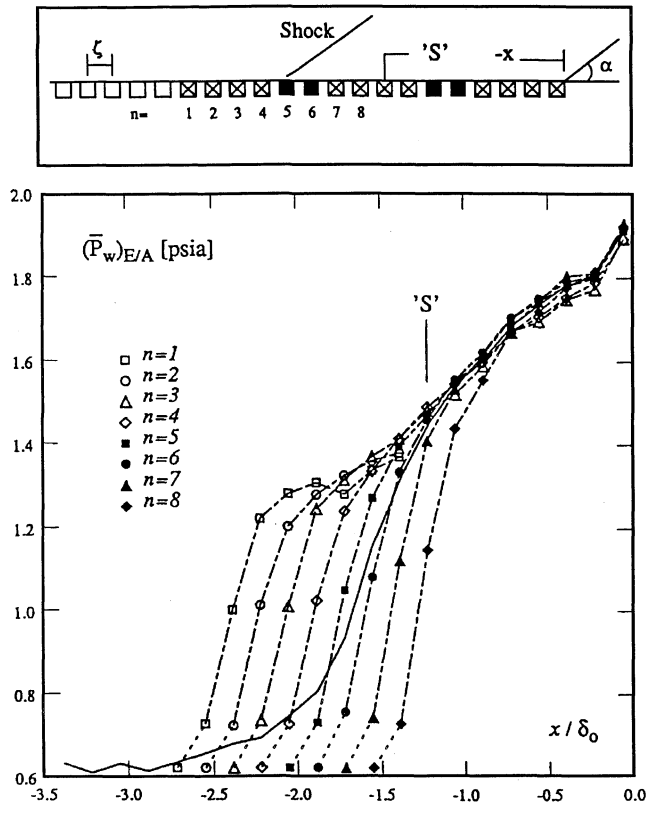

Fig. 10 Ensemble-averaged wall pressures upstream of the corner in a 28-deg, Mach 5 compression ramp interaction (figure from Ref. 16).

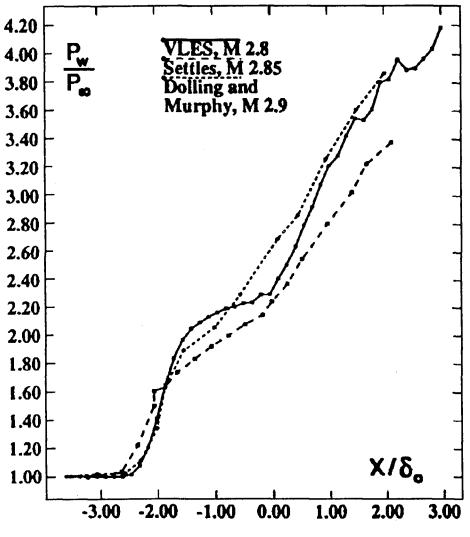

Fig. 11 Mean wall distribution (24-deg, Mach 3 compression ramp) predicted by large eddy simulation (figure from Ref. 18).

was used with Moin and Kim's two-part eddy viscosity model[19] as a subgrid scale model. Hunt and Nixon[18] note that it was not their intention "to supersede conventional simulations in accuracy but to gain insights that would enhance them." Thus, the simulation only "includes sufficient detail to reproduce the qualitative features of the shock oscillation and to give confidence in the accuracy of the simulation."[18] The predicted mean wall pressure distribution (Fig. 11) is certainly no better than that of Wilcox in Fig. 7d. However, the initial mean pressure rise is generated by the unsteady separation shock wave, as occurs in the experiment. Further, the computation is able to predict quantities, i.e., shock frequency and wall pressure rms, which had not been predicted at all by the previous Reynolds-averaged approaches.

Other than the large eddy simulation, none of the computational methods discussed earlier calculates the unsteadiness and, thus, it is not entirely surprising that results upstream of the corner are generally poor. The large eddy simulation is able to predict rms pressures (Fig. 12) and the separation shock zero-crossing frequency (Fig. 13). As seen, the rms peak upstream of the corner is overpredicted. However, the shock frequency is certainly of the right order of magnitude, as is the length scale of the streamwise region over which it translates. The latter led Hunt and Nixon[18] to conclude that this "suggests that the same mechanism causes the shock oscillations captured by the simulation as those observed experimentally." This suggestion may be correct, but in the current author's view it is probably too early to make such a statement. There are contradictions between certain findings in the simulations (notably the cause of the low-frequency, large-scale expansion/contraction of the separated flow), and neither experiment nor simulation presents a truly convincing argument supported by data.

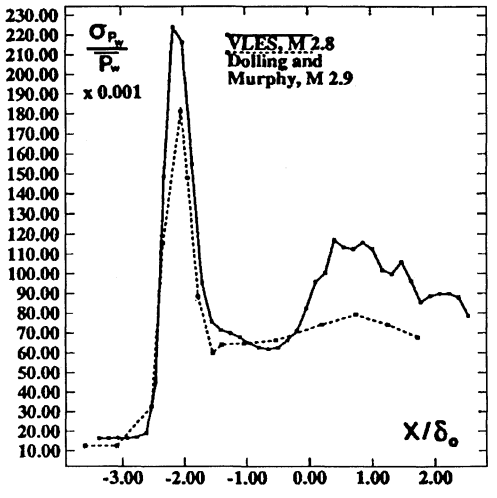

Fig. 12 Wall pressure standard deviation distribution (24-deg, Mach 3 compression ramp) predicted by large eddy simulation (figure from Ref. 18).

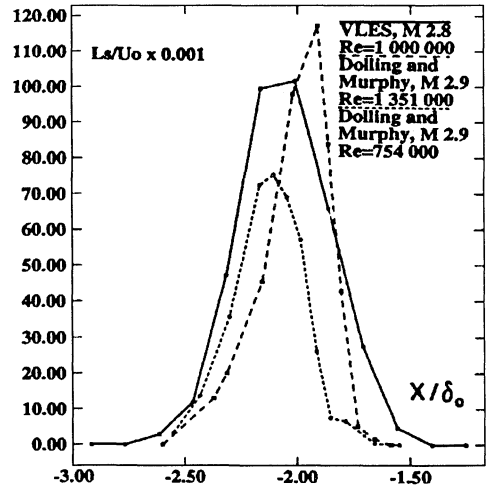

Fig. 13 Separation shock zero-crossing frequency (24-deg, Mach 3 compression ramp) predicted by large eddy simulation (figure from Ref. 18).

Experimental Separation Lines

Earlier, Horstman[6] was quoted as saying that one of the quantities of interest to the designer is the length of the separation zone. Experimentally, flow visualization is widely used in high-speed flows to find separation lines or lines of coalescence. Codes are frequently assessed on their ability to predict the location of these lines, as well as the separated-flow length scale, which is the distance from this line to reattachment. In flows in which the separation shock is unsteady, the physical meaning of these surface tracer lines naturally comes into question. Figure 14 shows a typical surface pattern in an interaction generated by a blunt fin together with wall pressure signals upstream of the separation line. It is quite evident that the

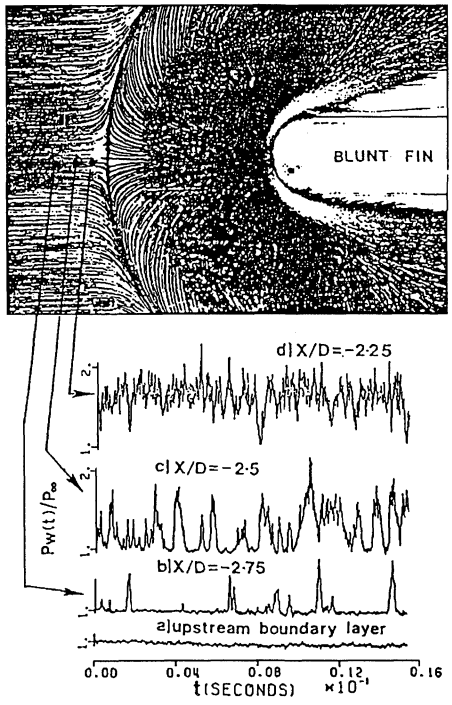

Fig. 14 Kerosene-lampblack surface flow visualization and wall pressure signals (figure from Ref. 21).

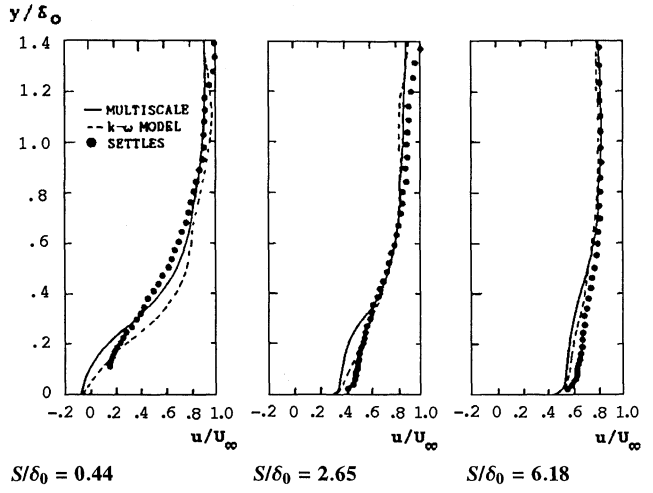

Fig. 15 Measured and computed mean velocity profiles downstream of the corner in a 24-deg, Mach 3 compression ramp interaction (figure from Ref. 14).

separation shock moves well upstream of what is referred to as the separation line.

In Refs. 20 and 21, conditional cross correlations of platinum thin-film signals and wall pressure fluctuations, respectively, were used to show that, in the case of an interaction induced by a circular cylinder in a Mach 5 turbulent boundary layer, the instantaneous separation point is at or close to the instantaneous shock foot in the intermittent region. Similar results were obtained in a 28-deg, Mach 5 compression ramp interaction.[22] The large eddy simulations show a similar result. Hence, the separation point itself also undergoes a large-scale, streamwise motion. The well-defined separation line from the kerosene-lampblack pattern (such as that in Fig. 14) is at or close to the downstream boundary of a region of intermittent separation.[20,21] The mean separation point (on the centerline) occurs at a shock foot intermittency of 50%, about $0.4D$–$0.5D$ upstream of the line of coalescence on the figure. Further, the relative location of the experimental line of coalescence of the surface streaks changes with interaction sweepback.[23] Results obtained in swept compression ramp interactions show that with increasing sweep the line of coalescence moves upstream in the intermittent region toward lower values of intermittency. A plausible explanation of why this occurs is given in Ref. 23.

Outgoing Mean Velocity Profiles

Frequently assessments are made of the ability of a code to predict the effects of the interaction on the outgoing velocity profile and the rapidity of its recovery. For example, in Ref. 14 Wilcox shows comparisons of the mean velocity profiles in the Mach 3, 24-deg compression ramp interaction, with predictions from the k–ω and multiscale turbulence models (Fig. 15). Downstream of the corner ($S/\delta_0 = 0.44$–6.18), the experimental data are much fuller than the computations below y/δ of about 0.4. Wilcox also computed the outgoing mean velocity profiles for Brown's experiment[24] of Mach 2.85 flow into a 30-deg axisymmetric compression corner. Below y/δ_0 of about 0.4, the measured profiles are much fuller than the computed profiles. Viegas et al.[11] also computed outgoing velocity profiles for the 20-deg compression ramp interaction of Settles[3] at Mach 2.8. The k–ε model was used, and results were presented based on both wall functions and integration to the wall. Again, the experimental profiles near the wall were fuller than the computed profiles.

McClure and Dolling[25] have examined how the outgoing mean pitot pressure profiles are actually generated in a Mach 5, 28-deg compression ramp interaction. Measurements were made using 1) a conventional pitot probe with a flattened tip with about 50 cm of pressure tubing between the probe tip and the pressure transducer and 2) a pitot probe with a single Kulite model XCQ-062-100A miniature pressure transducer projecting upstream of the tip. The frequency response of the Kulite probe was about 50 kHz. Three cases were studied: 1) ramp with suction applied along a 6-mm-long slot spanning the ramp near the reattachment, 2) ramp with suction slot exposed to the flow but without suction applied, and 3) baseline case, i.e., no slot or suction.

Results at four stations downstream of the corner are shown in Fig. 16 for the baseline and suction cases. Note that z is measured perpendicular to the ramp face. The solid lines are the mean profiles from the conventional probe. The dashed lines are frozen pitot profiles, which were obtained by averaging pitot pressure values only for the condition when the separation shock was located between two specified surface transducers. The intermittencies of the surface transducer pair used are indicated in the figure keys. The two positions correspond to the separation shock far upstream and downstream. Also indicated is the mean value from the fluctuating measurements.

It can be seen that, as the separation shock moves downstream (to a location of higher intermittency), the downstream extent of the interaction shrinks, and vice versa. This breathing behavior is consistent with the conclusions of Kussoy et al.[26] based on conditional laser Doppler measurements in a flared cylinder interaction and by Gramann and Dolling[27] based on conditional fluctuating-surface-pressure cross correlations on the face of a two-dimensional compression corner.

Comparison of the values from the conventional pitot probe with mean values of the fluctuating pitot pressure signal shows differences at each station. The differences have three possible causes. First, slight shifts in survey position show up as differences in pitot pressure. However, it is estimated that streamwise probe placement varied by less than 0.06δ between conventional and fluctuating runs and so should contribute only very slightly to P_t discrepancies. Second, the diameter of the fluctuating probe tip was 2.5 times greater than the conventional probe height, which would tend to integrate P_t over a larger distance and, hence, contribute to differences, particularly in regions of large gradients. It is probable that this integration has some effect. The third cause, which is almost certainly the major contributor, is the skewness of the fluctuating signal. Examination of the probability density distributions for the fluctuating pitot signals shows that, close to the ramp surface ($<0.6\delta_0$), they had positive skewness and, in some cases, exhibited a bimodal shape with very large separation between peak values (~32 psi). When the probability density values of these peaks were sufficiently different, the conventional pitot reading was higher than the mean of the fluctuations. Figure 17 shows this effect for the data set with the largest disagreement, the suction survey $X/\delta_0 \sim 1.45$. The accompanying probability distributions for the fluctuating pitot pressure clearly show

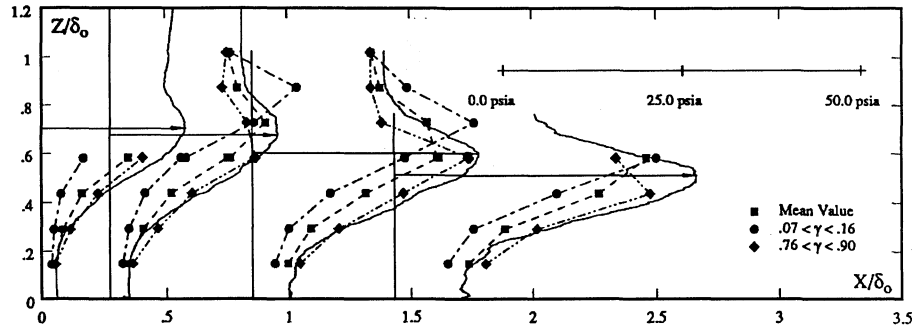

a) Baseline

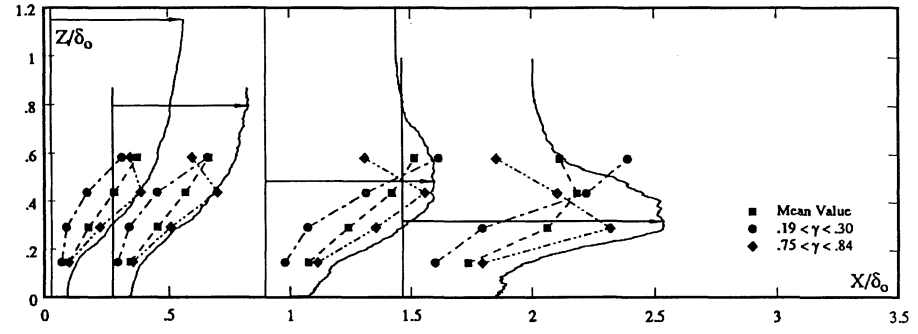

b) Ramp with suction (from Ref. 25)

Fig. 16 Mean and fluctuating pitot surveys downstream of the corner in a 28-deg, Mach 5 compression ramp interaction.

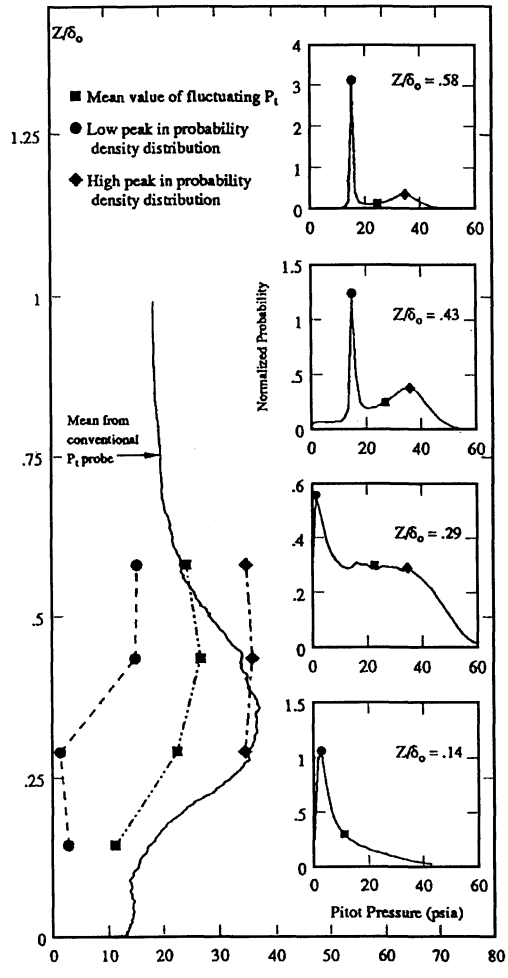

Fig. 17 Comparison of mean values from fluctuating and conventional mean pitot surveys (figure from Ref. 25).

that the conventional pitot probe measurement is biased toward the higher mode in the fluctuating pitot pressure data for $X/\delta_0 \leq 0.43$. This behavior reverses, though, for $Z/\delta_0 = 0.58$, where the probability density of the lower mode is six times greater than that of the higher mode. The 50 cm of tubing between the orifice and pressure transducer for the conventional pitot probe behaves as a pressure-sensitive filter with an output dependent on the nature of the fluctuations, i.e., frequency and amplitude content. The fundamental question is which distribution should be used for comparison with CFD.

Implications for Computation

The preceding results help explain how some of the time-averaged properties are generated. It is the occasional presence of the unsteady shock at the upstream influence (UI) line that first increases the mean pressure above the undisturbed value. Most of the time the pressure at UI is within the undisturbed range typical of the incoming boundary layer. The mean pressure rises downstream of UI because the translating shock spends an increasing amount of time upstream of stations nearer the separation line. Between UI and S, the abrupt pressure rise across the separation shock is smeared out in the time-averaged picture by the shock motion. The same physics, but with different characteristic length scales and frequencies, is seen in a wide variety of two- and three-dimensional, shock-induced separated flows.[15]

Modeling the flowfield with a stationary separation shock cannot simultaneously generate the correct upstream influence (as usually defined) and the correct time-averaged wall pressure. Even if the upstream influence matches the experiment (as it does in several of the computations in Fig. 7), the pressure distribution is generally incorrect. The stationary shock model essentially produces an instantaneous snapshot of the flowfield, i.e., the equivalent of one of the many shock-frozen distributions of Fig. 10, whereas, in the experiment, the mean pressure at any given point is the weighted average of a series of instantaneous flowfields, each for the separation shock at a different streamwise position. Because of this expansion/contraction of the separated flow, the outgoing boundary layer undergoes a relatively low-frequency flapping motion. The result is that the pitot pressure at a given station can undergo extremely

large variations (up to almost twice the freestream pitot pressure) and have a bimodal distribution. Whether this behavior is peculiar to the nominally two-dimensional ramp interaction or occurs in similar (or milder) form in other flows is not clear. The author is not aware of any detailed measurements. What is clear is that in a given flow different measuring techniques will provide different mean values. This is an issue that both the experimental and CFD practitioner should be aware of when presenting data for validation or when carrying out validation exercises.

As noted by one of the reviewers of this paper, a key question is as follows. At what stage does unsteadiness become sufficiently important that it must be included in the modeling? The answer is not clear-cut, and, as was also noted by the reviewer, probably depends on the application. If a code is to be used to explore fundamental flow physics, then including the unsteadiness is probably critical. On the other hand, for calculations in support of engineering design, where execution speed and low cost are important, an uncertainty of a boundary-layer thickness in separation location may be acceptable and unsteadiness ignored. However, note that, although δ is the appropriate length scale for the unsteadiness in compression ramp interactions, that is not the case in other flows. In upswept blunt fin interactions, the appropriate length scale is the leading-edge diameter D, and D may range from a fraction of δ to tens of δ. Further, it is not yet clear what role unsteadiness plays in determining the maximum heating rate, one of the most important quantities in high-speed flow. Although there is evidence that turbulence model corrections can result in radically improved predictions of heating rate, it is not clear whether such results are firmly rooted in the dominant physics. In the final analysis, it is up to the user to decide whether ignoring unsteadiness is acceptable. To assist a user in making such a judgment, some knowledge of how time-averaged data are generated is essential. The latter was the intent of this paper.

Summary

Experimental data have been presented that show how the time-averaged wall pressure and outgoing pitot pressure profiles are generated in a separated unswept compression ramp interaction. The dominant flowfield feature is the large-scale, low-frequency expansion/contraction of the separated flow. It has been shown that this unsteadiness plays a critical role in determining time-averaged wall pressures, the locations of separation on surface flow visualization images, and the outgoing boundary-layer velocity profiles. Without modeling the unsteadiness, accurate predictions of these and other quantities will likely remain elusive, irrespective of the turbulence model.

References

[1]Mehta, U. B., "Guide to Credible Computer Simulations of Fluid Flows," *Journal of Propulsion and Power*, Vol. 12, No. 5, 1996, pp. 940–948.

[2]Jameson, A., "Universities Foster CFD Growth," *Aerospace America*, Feb. 1992, pp. 42–47.

[3]Settles, G. S., "An Experimental Study of Compressible Turbulent Boundary Layer Separation at High Reynolds Numbers," Ph.D. Dissertation, Aerospace and Mechanical Sciences Dept., Princeton Univ., Princeton, NJ, Sept. 1975.

[4]Coleman, G. T., "A Study of Hypersonic Boundary Layers over a Family of Axisymmetric Bodies at Zero Incidence: Preliminary Report and Data Tabulation," Imperial College of Science and Technology, Aero Rept. 73-06, London, Sept. 1973.

[5]Coleman, G. T., and Stollery, J. L., "Heat Transfer in Hypersonic Turbulent Separated Flow," Imperial College of Science and Technology, Aero Rept. 72-05, London, March 1972.

[6]Horstman, C. C., "Prediction of Hypersonic Shock Wave/Turbulent Boundary Layer Interaction Flows," AIAA Paper 87-1367, June 1987.

[7]Holden, M. S., "Experimental Studies of Quasi-Two-Dimensional and Three-Dimensional Viscous Interaction Regions Induced by Skewed-Shock and Swept-Shock Boundary Layer Interaction," AIAA Paper 84-1677, June 1984.

[8]Coakley, T. J., and Huang, P. G., "Turbulence Modeling for High Speed Flows," AIAA Paper 92-0436, Jan. 1992.

[9]Coakley, T. J., Horstman, C. C., Marvin, J. G., Viegas, J. R., Bardina, J. E., Huang, P. G., and Kussoy, M. I., "Turbulence Compressibility Corrections," NASA TM 108827, May 1994.

[10]Viegas, J. R., and Horstman, C. C., "Comparison of Multi-Equation Turbulence Models for Several Shock Boundary Layer Interaction Flows," *AIAA Journal*, Vol. 17, No. 8, 1979, pp. 811–820.

[11]Viegas, J. R., Rubesin, M. W., and Horstman, C. C., "On the use of Wall Functions as Boundary Conditions for Two-Dimensional Separated Compressible Flows," AIAA Paper 85-0180, Jan. 1985.

[12]Dolling, D. S., and Murphy, M. T., "Unsteadiness of the Separation Shock Wave Structure in a Supersonic Compression Ramp Flowfield," *AIAA Journal*, Vol. 21, No. 12, 1983, pp. 1628–1634.

[13]Champney, J., "Modeling of Turbulence for Compression Corner Flows and Internal Flows," AIAA Paper 89-2344, July 1989.

[14]Wilcox, D. D., "Supersonic Compression Corner Applications of a Multi-Scale Model for Turbulent Flows," *AIAA Journal*, Vol. 28, No. 7, 1990, pp. 1194–1198.

[15]Dolling, D. S., "Fluctuating Loads in Shock Wave/Turbulent Boundary Layer Interaction," AIAA Paper 93-0284, Jan. 1993.

[16]Erengil, M. E., and Dolling, D. S., "Separation Shock Motion and Ensemble-Averaged Wall Pressures in a Mach 5 Compression Ramp Interaction," *AIAA Journal*, Vol. 29, No. 5, 1991, pp. 728–735.

[17]Hunt, D. L., "An Investigation of Supersonic Buffet Using a Large Eddy Simulation," Ph.D. Dissertation, Dept. of Aeronautical Engineering, Queen's Univ. of Belfast, Belfast, Northern Ireland, UK, Sept. 1995.

[18]Hunt, D. L., and Nixon, D., "A Very Large Eddy Simulation of an Unsteady Shock Wave/Turbulent Boundary Layer Interaction," AIAA Paper 95-2212, June 1995.

[19]Moin, P., and Kim, J., "Numerical Investigation of Turbulent Channel Flow," *Journal of Fluid Mechanics*, Vol. 118, 1982, pp. 341–377.

[20]Gramann, R. A., and Dolling, D. S., "Interpretation of Separation Lines from Surface Tracers in Shock Induced Turbulent Flow," *AIAA Journal*, Vol. 25, No. 12, 1987, pp. 1545, 1546.

[21]Gramann, R. A., and Dolling, D. S., "Detection of Turbulent Boundary Layer Separation Using Fluctuating Wall Pressure Signals," *AIAA Journal*, Vol. 28, No. 6, 1990, pp. 1052–1056.

[22]Gramann, R. A., "Dynamics of Separation and Reattachment in a Mach 5 Unswept Compression Ramp Flow," Ph.D. Dissertation, Dept. of Aerospace Engineering and Engineering Mechanics, Univ. of Texas, Austin, TX, Dec. 1989.

[23]Erengil, M. E., and Dolling, D. S., "Effects of Sweepback on Unsteady Separation in Mach 5 Compression Ramp Interactions," AIAA Paper 92-0430, Jan. 1992.

[24]Brown, J. D., "Two Component LDV Investigation of Shock Related Turbulent Boundary Layer Separation with Increasing Three-Dimensionality," Ph.D. Thesis, Univ. of California, Berkeley, CA, 1986.

[25]McClure, W. B., and Dolling, D. S., "Exploratory Study of Effects of Suction Near Reattachment on the Unsteadiness of a Mach 5 Compression Ramp Interaction," AIAA Paper 91-1767, June 1991.

[26]Kussoy, M. I., Brown, J. D., Brown, J. L., Lockman, W. K., and Horstman, C. C., "Fluctuations and Massive Separation in Three-Dimensional Shock-Wave/Boundary-Layer Interactions," 2nd International Symposium on Transport Phenomena in Turbulent Flows, Univ. of Tokyo, Tokyo, Japan, Oct. 1987.

[27]Gramann, R. A., and Dolling, D. S., "Dynamics of Separation and Reattachment in a Mach 5 Unswept Compression Ramp Flow," AIAA Paper 90-0380, Jan. 1990.

C. G. Speziale
Associate Editor